ARMY RESEARCH LABORATORY

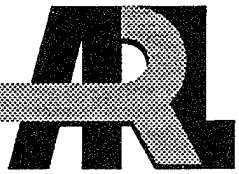

Euler and Navier-Stokes Simulations of Shock Wave Interaction With a Generic Block Target

Stephen J. Schraml
Dixie M. Hisley

ARL-TR-848 September 1995

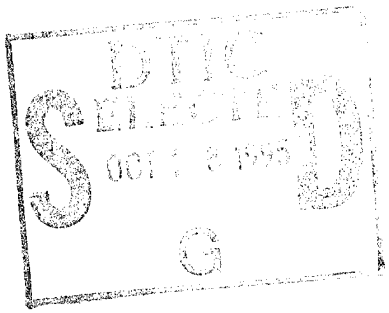

NOTICES

Destroy this report when it is no longer needed. DO NOT return it to the originator.

Additional copies of this report may be obtained from the National Technical Information Service, U.S. Department of Commerce, 5285 Port Royal Road, Springfield, VA 22161.

The findings of this report are not to be construed as an official Department of the Army position, unless so designated by other authorized documents.

The use of trade names or manufacturers' names in this report does not constitute indorsement of any commercial product.

REPORT DOCUMENTATION PAGE

Form Approved
OMB No. 0704-0188

1. AGENCY USE ONLY *(Leave blank)*	2. REPORT DATE	3. REPORT TYPE AND DATES COVERED
	September 1995	Final, January - November 1992

4. TITLE AND SUBTITLE

Euler and Navier-Stokes Simulations of Shock Wave Interaction with a Generic Block Target

5. FUNDING NUMBERS

4G592542U2202U

6. AUTHOR(S)

Stephen J. Schraml, Dixie M. Hisley

7. PERFORMING ORGANIZATION NAME(S) AND ADDRESS(ES)

U.S. Army Research Laboratory
ATTN: AMSRL-WT-NC
Aberdeen Proving Ground, MD 21005-5066

8. PERFORMING ORGANIZATION REPORT NUMBER

ARL-TR-848

9. SPONSORING/MONITORING AGENCY NAMES(S) AND ADDRESS(ES)

10.SPONSORING/MONITORING AGENCY REPORT NUMBER

11. SUPPLEMENTARY NOTES

12a. DISTRIBUTION/AVAILABILITY STATEMENT

Approved for public release; distribution is unlimited.

12b. DISTRIBUTION CODE

13. ABSTRACT *(Maximum 200 words)*

A series of numerical simulations of blast wave/target interaction was performed to match a series of experiments conducted at the Centre d'Etudes de Gramat (CEG), France. The experiments that were modeled involved a square, two-dimensional block target positioned in the vertical center of a shock tube test section and subjected to non-decaying blast waves of various amplitudes. The results of the inviscid second order hydrodynamic advanced research code (SHARC) and the viscous USA-RG2 code simulations are compared to experimentally measured pressure histories. Particular emphasis is placed on the accurate modeling of vortex formation and evolution, which influences the aerodynamic loading of the target. The viscous and inviscid results are directly compared to determine the most accurate method of modeling both diffraction and drag phase blast loading of targets.

14. SUBJECT TERMS

gas dynamics, blast waves, computational fluid dynamics, shock tubes, turbulence

15. NUMBER OF PAGES

31

16. PRICE CODE

17. SECURITY CLASSIFICATION OF REPORT	18. SECURITY CLASSIFICATION OF THIS PAGE	19. SECURITY CLASSIFICATION OF ABSTRACT	20. LIMITATION OF ABSTRACT
UNCLASSIFIED	UNCLASSIFIED	UNCLASSIFIED	SAR

Intentionally Left Blank

Acknowledgments

The authors wish to acknowledge the assistance of Didier Tournemine of the Centre d'Etudes de Gramat, France, for providing the experimental data and initial inviscid calculation results through Defence Exchange Agreement MWDDEA-A-80-F-1265.

Mr. Richard J. Pearson performed a technical review of this report and provided many useful comments to clarify and improve the presentation of the work that is described.

Intentionally Left Blank

Table of Contents

		Page
	Acknowledgments	iii
	List of Figures	vii
1.	Introduction	1
2.	Shock Tube Facility	1
3.	Description of Flow Solvers	3
4.	Experimental and Computational Results	4
5.	Summary	7
	References	19
	Distribution List	21

Intentionally Left Blank

List of Figures

Figure		Page
1	Schematic Diagram of Zephire Test Section	8
2	$M_s = 1.165$, Front Face, SHARC: First Order, 522x294 Grid	8
3	$M_s = 1.165$, Rear Face, SHARC: First Order, 522x294 Grid	9
4	$M_s = 1.165$, Top Face, SHARC: First Order, 522x294 Grid	9
5	$M_s = 1.265$, Front Face, SHARC: First Order, 522x294 Grid	10
6	$M_s = 1.265$, Rear Face, SHARC: First Order, 522x294 Grid	10
7	$M_s = 1.265$, Top Face, SHARC: First Order, 522x294 Grid	11
8	$M_s = 1.362$, Front Face, SHARC: First Order, 522x294 Grid	11
9	$M_s = 1.362$, Rear Face, SHARC: First Order, 522x294 Grid	12
10	$M_s = 1.362$, Top Face, SHARC: First Order, 522x294 Grid	12
11	$M_s = 1.362$, Top Face, SHARC: Second Order, 522x294 Grid	13
12	$M_s = 1.362$, Top Face, SHARC: Second Order, 522x652 Grid	13
13	$M_s = 1.362$, Top Face, SHARC: Second Order, 958x1072 Grid	14
14	$M_s = 1.362$, Front Face, USA-RG2, Laminar-Viscous	14
15	$M_s = 1.362$, Rear Face, USA-RG2, Laminar-Viscous	15
16	$M_s = 1.362$, Top Face, USA-RG2, Laminar-Viscous	15
17	$M_s = 1.362$, Top Face, USA-RG2, B-L Turbulence	16
18	$M_s = 1.362$, Top Face, USA-RG2, k-L Turbulence	16
19	$M_s = 1.362$, Top Face, USA-RG2, k-ϵ Turbulence	17

Intentionally Left Blank

1. Introduction

To study the phenomenology of nuclear blast loading on military equipment, laboratory shock tubes are sometimes configured to produce simulations of nuclear blast waves. The laboratory environment can provide pressure measurements on surfaces of bodies as well as a means of characterizing the flow field through optical techniques. One laboratory shock tube facility, called Zephire, is located at the Centre d'Etudes de Gramat (CEG), France. The limitation of this laboratory facility is that only simplified, subscale targets can be studied in its environment. To provide a more complete representation of the phenomena, numerical simulation techniques are sometimes employed. These techniques allow more detailed data (density, velocity, dynamic pressure) to be collected in critical areas of interest.

In addition to supplementing experimental data, numerical simulations of blast wave-target interaction can be used to directly model the effects of nuclear blast on tactical equipment. With the rising cost of full scale experimentation and the increasing performance of supercomputers, coupled numerical simulation of blast loading and rigid body response may become an economical method of determining the vulnerability of equipment to nuclear blast effects.

To predict the response of targets to nuclear blast loading, one must first accurately model the aerodynamic loads applied to the targets. Controlled laboratory experiments, such as those performed in the Zephire facility, provide an excellent means of validating the presently employed computational fluid dynamics (CFD) algorithms. This method of validation will also ensure that the most appropriate algorithm is used in high-resolution, three-dimensional (3-D) calculations of blast loading on complex, moving bodies.

2. Shock Tube Facility

The Zephire shock tube facility is operated by CEG for the purpose of studying shock waves and their interactions with targets.[1] The facility can also be used to develop and test measuring equipment and to study possible modifications of larger blast simulation facilities.

The Zephire shock tube is composed primarily of 0.5 m diameter tube sections, each of which is 1 m long. The total maximum length of the shock tube is 45 m. As many as 10 tube sections, each of which is 1 m in length, may be used to construct the driver section for a given experiment. The actual number of tube sections used to construct the driver depends on the desired blast wave characteristics. The expansion section of this facility is also composed of these 0.5 m diameter tube sections and can be a maximum of 35 m long. The driver and expansion sections are separated by a thin diaphragm, which is ruptured with heating wires.

Within the expansion section a test section exists for studying the interactions of shock waves with targets. The center of the test section is located at a position 15 m downstream from the diaphragm. A schematic diagram of the test section positioned within the expansion section is illustrated in Figure 1. The test section is rectangular and has a knife-edged leading

surface that allows the shock wave to enter the test section with minimum disturbance. As illustrated in the figure, the test section has a height of 323 mm, a width of 282 mm, and a total length of 3300 mm between the upstream and downstream knife edges.

Zephire is an excellent facility for studying shock wave-target interactions because it is equipped with high-speed cameras for visualizing the flow during the diffraction and drag phases. Combining these optical data with pressure histories measured on the faces of the target provides detailed information about the evolution of the flow field in the vicinity of the target. In the experiments discussed here, the target employed was a 70 mm by 70 mm block positioned near the vertical center of the test section. This target is also illustrated in Figure 1. Mounted within the target were three pressure gauges that were used to measure pressure histories on the faces of the target. One gauge was mounted in the center of the front face. Another was positioned in the center of the rear face. The third gauge was mounted in the top face of the target, centered at a distance of 31 mm from the upstream edge of the target.

The numerical simulations presented in this paper correspond to three experiments performed in Zephire. These experiments involved the interaction of the block target with non-decaying blast waves of various incident static overpressure amplitudes. The conditions of each experiment are described in Table 1.

Table 1. Conditions of Experiments

	Shot Number		
	1	2	3
Atmospheric Conditions			
Temperature (K)	294.5	294.1	295.8
Pressure (kPa)	97.8	97.3	96.9
Density (kg/m^3)	1.157	1.153	1.141
Shock Properties			
Shock Velocity (m/s)	400.8	434.9	469.6
Shock Mach Number	1.165	1.265	1.362
Conditions Behind Shock			
Static Overpressure (kPa)	40.5	67.8	96.3
Temperature (K)	325.6	343.5	363.7
Density (kg/m^3)	1.479	1.673	1.849
Particle Velocity (m/s)	87.4	135.3	179.7

These experiments were modeled in a series of calculations performed with the second order, hydrodynamic, advanced research code (SHARC) and the universal solution algorithms, real gas, 2-D (USA-RG2) code. A description of each code is provided, followed by a discussion of the results obtained from the numerical simulations.

3. Description of Flow Solvers

Two different computational fluid dynamics codes were used to model the Zephire experiments. The first was SHARC, an explicit Euler solver[2] and is a derivative of the HULL code which was originally developed at the U.S. Air Force Weapons Laboratory for the purpose of modeling nuclear blast loading on missile silos.[3]

SHARC is a finite difference code that employs a rectangular discretized mesh to model the computational domain. The code supports 2-D axisymmetric, 2-D cartesian and 3-D cartesian geometries. Variable spacing of grid points along each coordinate axis is allowed. Complex shapes are modeled by placing a perfectly rigid, perfectly reflective material, known as "island" material, in the rectangular (2-D) or box shaped (3-D) computational cells. The degree to which computational results match experimental results is affected by the grid resolution used. In general, higher grid resolutions lead to better agreement. Increasing grid resolution, however, can quickly lead to unreasonably long run times. The grid resolution selected for a computational study involves a trade off between the accuracy of the result and CPU time.

Early versions of SHARC employed a solution algorithm that was first order accurate in space and time. Later, a second order accurate solution algorithm was added to reduce the diffusiveness of the solution. Another improvement to the SHARC code was the addition of a $k-\epsilon$ turbulence model, which improves the capability of the code in cases that involve shear flow.[4] An artificial viscosity model is also available in the SHARC code. This model can be used as a damping mechanism to minimize the effects of "overshoots" near shock fronts. Even with the artificial viscosity model, SHARC is still an inviscid code. That is, the algorithm in SHARC is a discretization of the Euler equations, a subset of the Navier-Stokes equations, which contain no viscous terms. Thus, SHARC is not capable of modeling the effects of boundary layers. Calculations of the shock-target interactions in the Zephire experiments were performed by SHARC using a variety of solver options and grid configurations. After the SHARC calculations were complete, a second set of computations was performed using Rockwell Science Center's USA-RG2 code.

The USA-RG2 code discretizes the Navier-Stokes equations using a finite volume, Roe's Riemann solver, total variation diminishing (TVD), implicit algorithm.[5] The implicit scheme produces an algorithm that is well suited for blast wave calculations[6] because upwind flux difference splitting with TVD achieves second order accuracy without introducing spurious oscillations near discontinuities. Strong gradients and complex flow fields are resolved accurately. TVD schemes are often referred to as modern shock-capturing methods because the numerical dissipation terms are nonlinear. That is, the amount of dissipation is controlled by automatic feedback mechanisms that can vary from one grid point to another. Also, the dissipation is scaled to the underlying eigensystem of the hyperbolic Euler equations. In classical shock capturing methods, the numerical dissipation terms are either linear so that the same amount of numerical dissipation is added at all grid points or the numerical dissipation is controlled by parameters that must be optimized. Classical shock capturing methods typically result in oscillatory solutions at strong discontinuities.

The conservative nature of the scheme captures shocks and other discontinuities automatically. The finite volume philosophy ensures conservation at interior grid points. The implicit version of the scheme requires more computations per integration step than the explicit version but permits larger time steps which, for mathematically stiff (viscous) problems, reduces computational expense. The code has the capability to handle multi-zone grids and has several turbulence models available. The turbulence models available are a modified Baldwin-Lomax[7] (0 equation), $k - L$[8] (1 equation), and $k - \epsilon$[9] (2 equation) models.

The USA-RG2 code and other computational fluid dynamics codes like it employ gridding techniques that are quite different from those of SHARC. In particular, the coordinate axes are not required to be straight lines. Rather, the coordinate axes can be defined in practically any form necessary to define the complex shape of the system being modeled. This type of grid is referred to as "body conformal" because the grid can be wrapped around the body of interest, thus modeling it with a high level of accuracy. An additional level of flexibility is available to the USA-RG2 code in that it supports multi-zone grids. This basically means that numerous independent body conformal grids can be combined in one computational model to represent the system with a high degree of fidelity without placing a large number of grid points in regions of uniform steady flows.

4. Experimental and Computational Results

The experiments that were performed in the Zephire shock tube were originally followed by a set of hydrocode calculations performed at CEG with an early version of the SHARC code. This version lacked some of the features that were described earlier. Most significantly, this early version of SHARC did not have the second-order accurate solution algorithm and the $k - \epsilon$ turbulence model.

These calculations were 2-D numerical simulations of the flow inside the test section of the Zephire shock tube. Thus, only the rectangular cross section, from the upstream knife edge of the test section to the downstream knife edge, was modeled. It was not necessary to model the circular cross section of the expansion section because the influence of flow disturbances originating from this part of the facility would not reach the target during the period of interest of the experiment. Because the target was positioned near the vertical center of the test section, only half of the flow field was modeled vertically, from the centerline of the target to the upper wall of the test section.

The calculations performed by CEG with this early version of SHARC employed a 522x294 grid and accurately reproduced the experimentally measured pressure histories for the 40.5 kPa and 67.8 kPa incident static overpressure experiments, as illustrated in Figures 2 through 7.

For the 96.8 kPa experiment, the front and rear surface pressure histories produced by SHARC were also a good match to the experimental data, as illustrated in Figures 8 and 9. However, Figure 10 shows that for the top face pressure history, there were significant differences between the experiment and the result of the early SHARC code.

Close examination of Figure 10 explains much about phenomena involved in the shock wave-target interaction. The initial interaction of the shock with the target causes the initial rise in the pressure history, which is followed by a plateau. Behind the primary shock, a vortex is formed at the leading edge of the target and travels downstream across the top face of the target. As this vortex passes over the pressure gauge, the pressure at the gauge begins to decrease. The amount of pressure decrease is a function of the amplitude of the primary shock. A stronger incident shock will generate a lower pressure within this vortex, and thus a greater pressure drop after the initial plateau in the top surface pressure history. This pressure drop, which is combined with a decrease due to a rarefaction wave from the downstream edge, is followed by two sharp increases. These pressure increases are caused by reflections from the top wall of the test section. It is here that the significant differences between the experiment and the calculation occur.

In an attempt to better understand the differences between the top face experimental and computational data for the 96.3 kPa incident static overpressure experiment, ARL performed a series of calculations with its version of the SHARC code. The ARL installation of SHARC contains all the features described earlier in this report. The first calculation employed the exact problem definition as the calculations performed by CEG. The only difference between this calculation and the CEG calculation was that the second order accurate solution algorithm was employed whereas the first order accurate scheme had been used in the CEG calculations. The top surface pressure history result for this calculation can be seen in Figure 11. The second order code results significantly deviate from the experiment starting at about 0.6 ms. Comparing this to Figure 10, one can see that after 0.6 ms, the deviation from the experimental pressure is larger than the first order result.

The second order SHARC calculations performed with the original CEG problem definition resolved the computational domain into a grid containing 522 points in the horizontal direction and 294 points in the vertical direction. As discussed earlier, the spacing between grid points may be varied in this type of finite difference calculation. This particular grid employed a constant grid point spacing of 0.25 mm in both the horizontal and vertical directions in the region close to the target and near the top wall of the test section. Between the top face of the target and the top wall of the test section, the grid point spacing was allowed to grow to a maximum of 2.6 mm. This increase in grid spacing was done in a effort to reduce the time required for the calculation to run. However, it was felt that some of the definition of the complex shock structure between the top face of the target and the top wall of the test section could be artificially dissipated in this region of coarse grid resolution. Consequently, another second order SHARC calculation was performed, which employed a grid with the same 522 grid points in the horizontal direction as the previous calculation, but with 652 grid points in the vertical direction. This new grid used a constant grid spacing of 0.25 mm for the entire vertical distance between the target centerline and the top wall of the test section. The top face pressure history for this calculation is compared to the experimental data in Figure 12. The result is basically the same as that of the 522x294 grid calculation, except that there is more activity near the end of the record.

Because the result of the 522x652 grid calculation showed no significant improvement over the 522x294 grid case, it was decided that the next logical means of refining the grid was to further decrease the size of the cells throughout the computational domain. A final SHARC calculation was performed in which a 958x1072 grid was employed. This calculation used grid point spacing of 0.10 *mm* near the target in the horizontal and vertical directions. The grid point spacing in the 958x1072 grid was allowed to grow to only 0.20 *mm* between the top face of the target and the top wall of the test section. The result of this calculation is illustrated in Figure 13. Comparing this figure to the previous SHARC results shows that the 958x1072 grid calculation provided the closest agreement to the experimental data. The 958x1072 grid SHARC calculation required nearly 100 CPU hours to complete on a single processor of a Cray XMP. SHARC calculations with further grid refinement than this were simply not possible due to the long run times which would be required. Therefore, this result is considered to be the best inviscid solution obtainable with the present class of vector supercomputers.

A final set of calculations using the USA-RG2 code was executed on a Cray 2 supercomputer. These calculations employed a 528x848 grid point, five zone grid in which the grid point spacing was 0.1 *mm* near the surface of the target in both horizontal and vertical directions, identical to the grid resolution near the target in the most highly resolved SHARC calculation. The first USA-RG2 calculation employed a laminar viscous solution scheme, thus assuming that the flow is viscous but nonturbulent and required 2.2 hours of CPU time to complete. The front and rear surface pressure histories for this calculation are compared to the experimental data in Figures 14 and 15, respectively. As with the SHARC results, the USA-RG2 code accurately predicts the flow histories on these surfaces.

The pressure history on the top surface of the target produced by the laminar viscous solution is presented in Figure 16. This figure shows that, until 0.5 milliseconds, the result closely follows the experimental pressure history for the top face of the target, after which, deviations from the experimental data exist.

Three additional USA-RG2 calculations were performed to model the influence of turbulence within the boundary layer. These calculations employed three different turbulence models that are available with the USA-RG2 code: Baldwin-Lomax, $k - L$, and $k - \epsilon$. The results of the calculations with these turbulence models are presented in Figures 17, 18, and 19. The result obtained from the calculation using the Baldwin-Lomax turbulence model, Figure 17, did not predict the pressure history as well as the laminar viscous calculation. The Baldwin-Lomax ran in 2.5 hours, and its result fell well below the minimum pressure following the decay caused by the vortex migration across the top surface.

Figure 18 shows that the calculation that employed the $k-L$ turbulence model accurately predicted the value of the minimum pressure, but following this minimum, the pressure history experienced a rapid increase. When compared to the experimental data, it appears that the reflections from the top wall of the test section arrive too soon in this calculation. This calculation was completed in 5 hours. Finally, the 17.3 hour calculation with the $k - \epsilon$ turbulence model is shown in Figure 19. The top face pressure history from this calculation closely follows the experimental data through the initial shock, the decay, and the minimum

before the first reflection from the top wall of the test section. Both the $k - L$ calculation and the $k - \epsilon$ calculation are improvements over the laminar viscous and Baldwin-Lomax turbulence calculations.

5. Summary

Experiments were conducted in the CEG Zephire shock tube facility to study the interaction of blast waves with a square, 2-D target. Calculations have been performed with an inviscid Euler solver, SHARC, and a full Navier-Stokes code, USA-RG2, to compare to these experiments. Particular emphasis has been placed on the ability of these codes to model the vortex formation and evolution processes that have a significant impact on the aerodynamic loading of surfaces that are parallel to the primary direction of flow. Validation of the computational results was accomplished through the comparison of experimentally measured pressure histories to those obtained from the numerical simulations. The use of a highly resolved grid, combined with a second order accurate solution algorithm, helped to bring the inviscid code result into better agreement with the experiment. However, the inviscid code was still unable to accurately model the flow along the top surface of the target during the drag phase. The four viscous solutions that were presented provided a better correlation to the experimental data, particularly in late time. Of these, the solutions that employed $k-L$ and $k-\epsilon$ turbulence models provided the most accurate simulation of the aerodynamic loading on the top surface of the target. These findings provide a valid argument for the inclusion of turbulent, viscous flow modeling in future 3-D numerical simulations of blast loading on military equipment.

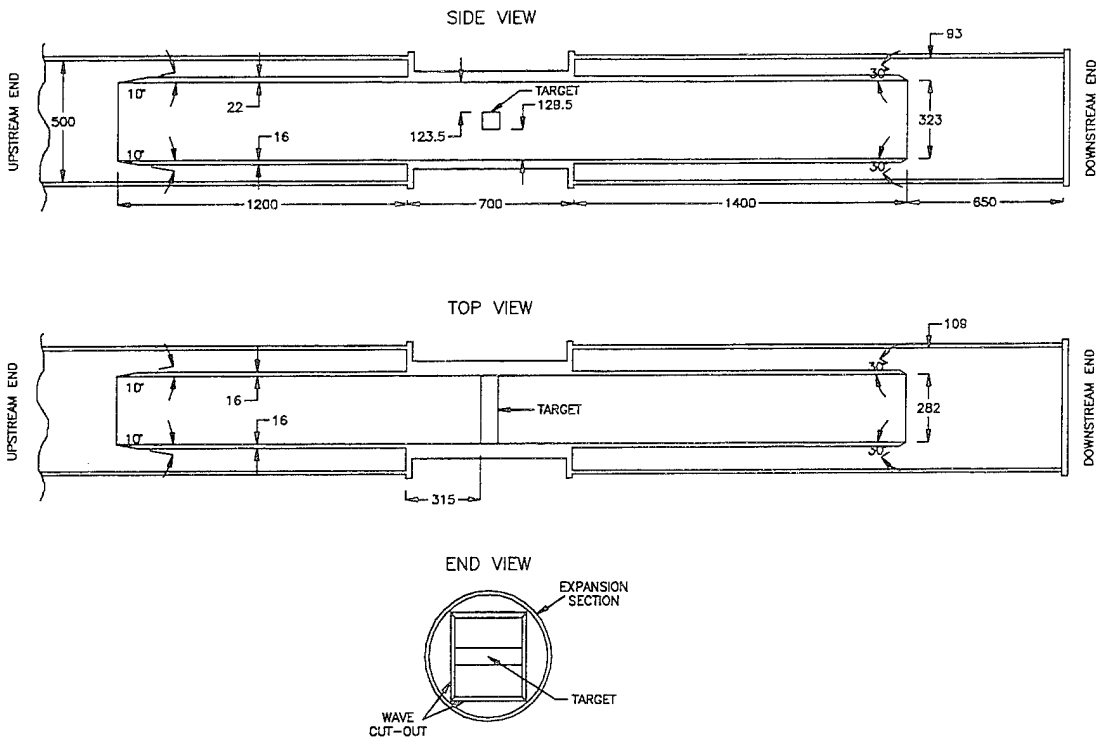

Figure 1. Schematic Diagram of Zephire Test Section

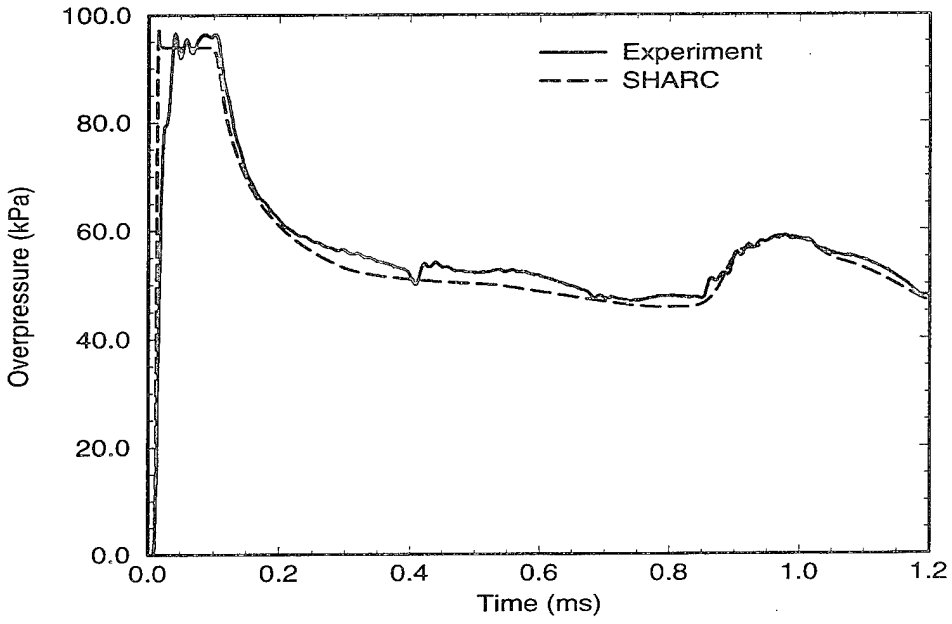

Figure 2. $M_s = 1.165$, Front Face, SHARC: First Order, 522x294 Grid

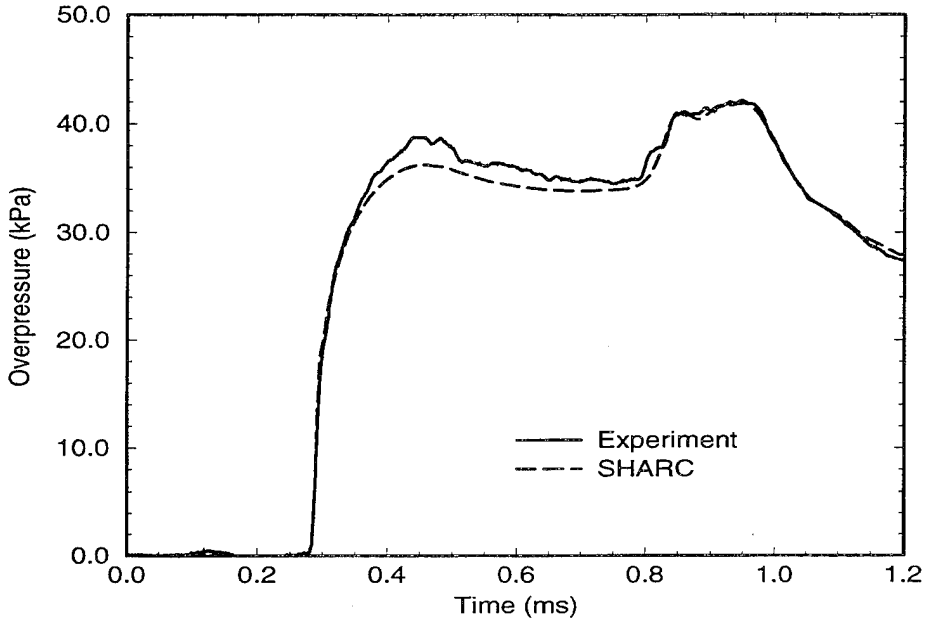

Figure 3. $M_s = 1.165$, Rear Face, SHARC: First Order, 522x294 Grid

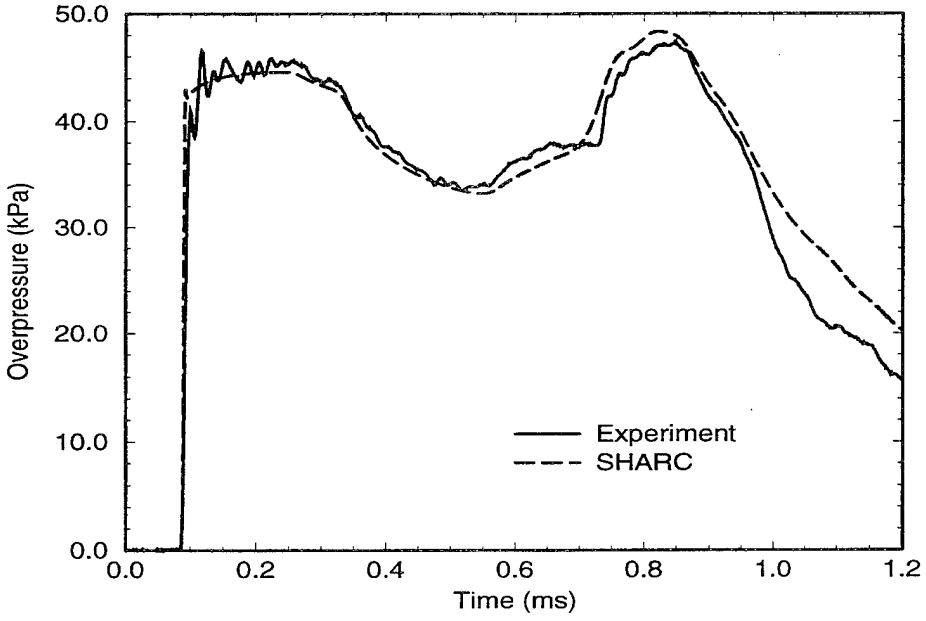

Figure 4. $M_s = 1.165$, Top Face, SHARC: First Order, 522x294 Grid

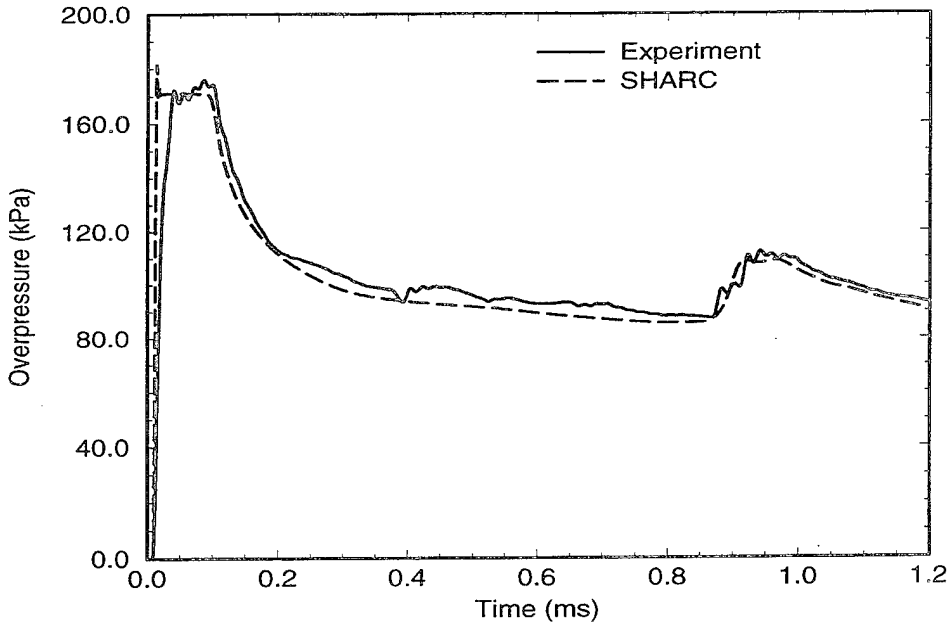

Figure 5. $M_s = 1.265$, Front Face, SHARC: First Order, 522x294 Grid

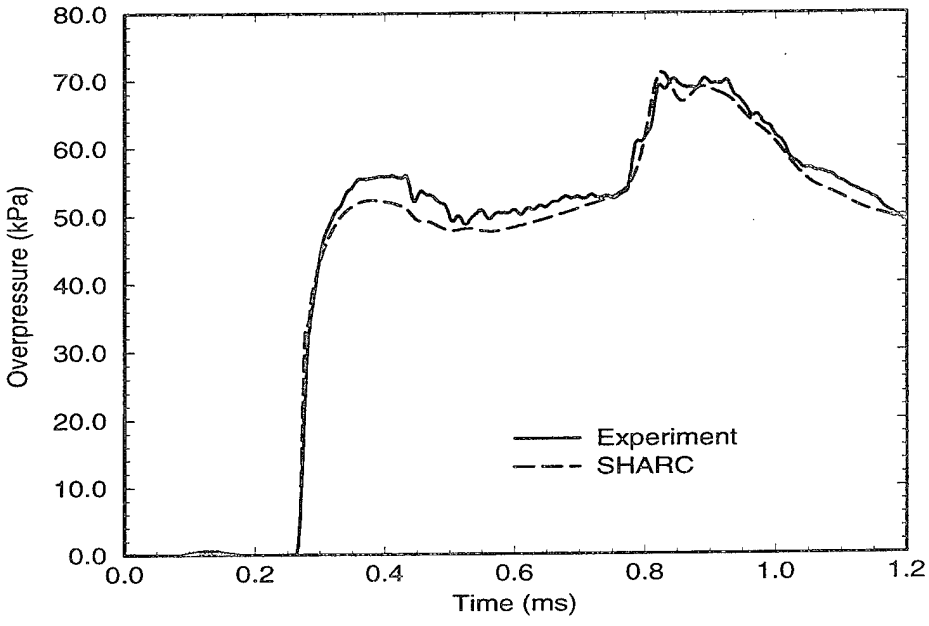

Figure 6. $M_s = 1.265$, Rear Face, SHARC: First Order, 522x294 Grid

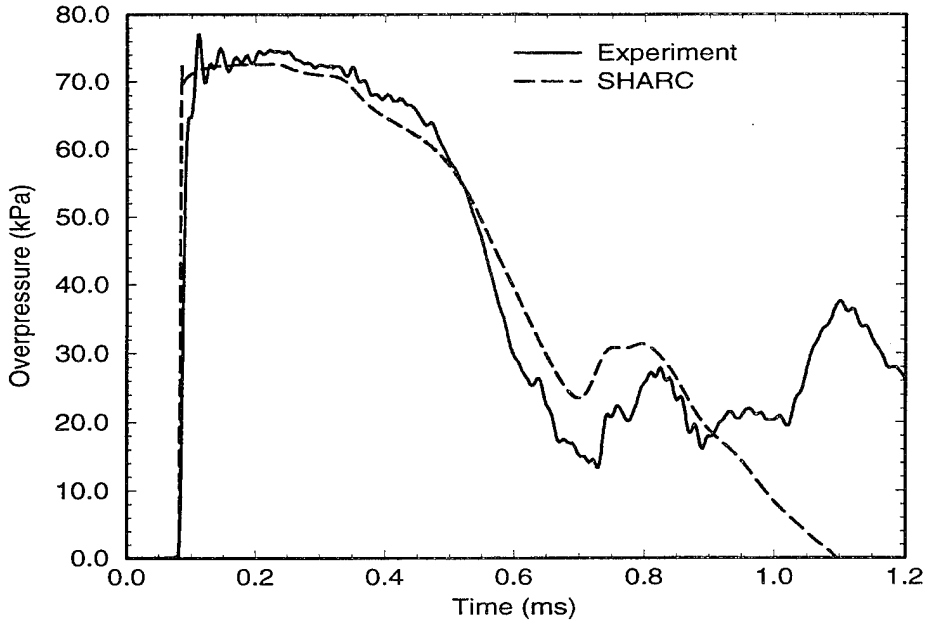

Figure 7. $M_s = 1.265$, Top Face, SHARC: First Order, 522x294 Grid

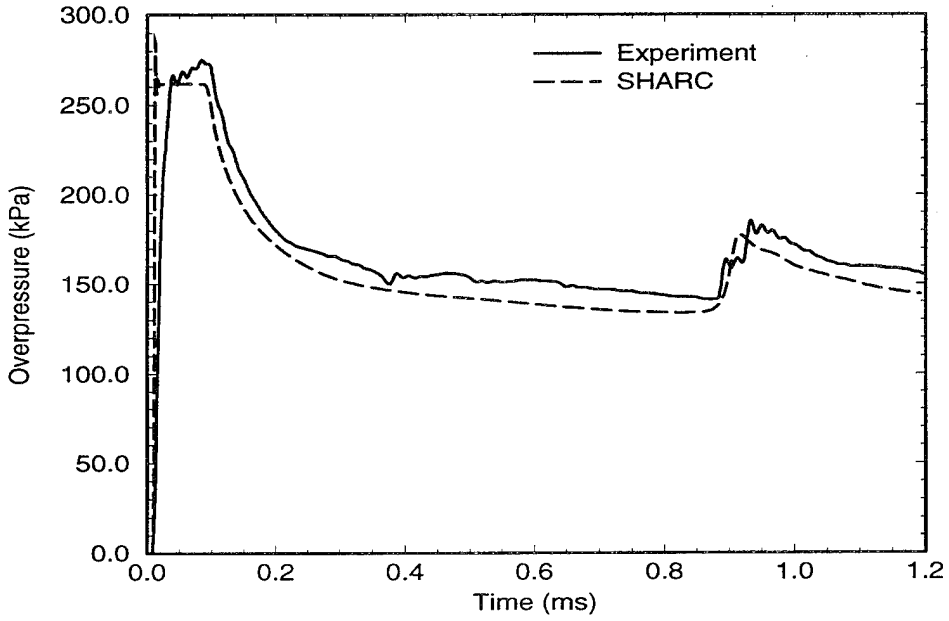

Figure 8. $M_s = 1.362$, Front Face, SHARC: First Order, 522x294 Grid

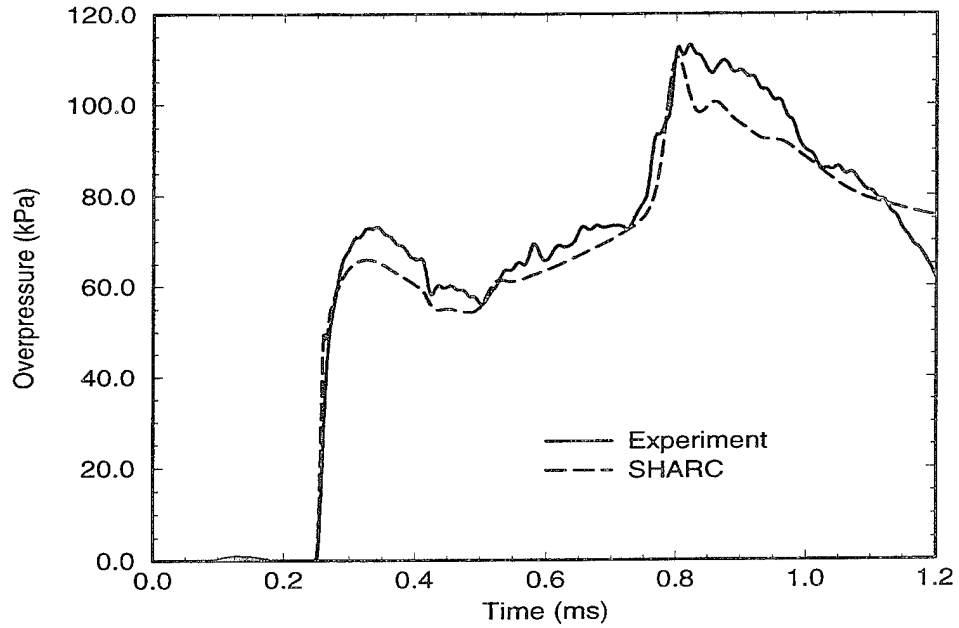

Figure 9. $M_s = 1.362$, Rear Face, SHARC: First Order, 522x294 Grid

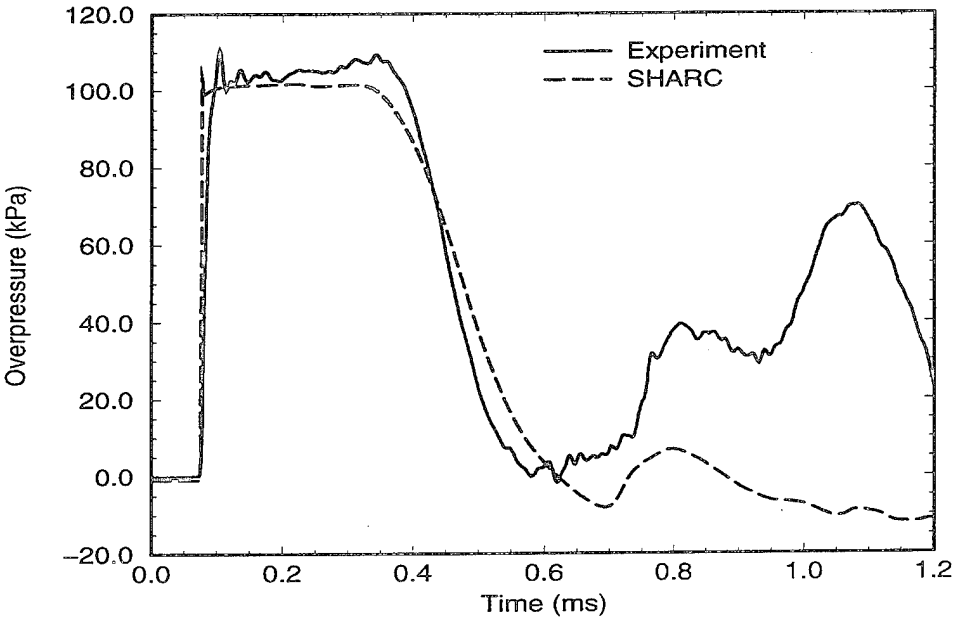

Figure 10. $M_s = 1.362$, Top Face, SHARC: First Order, 522x294 Grid

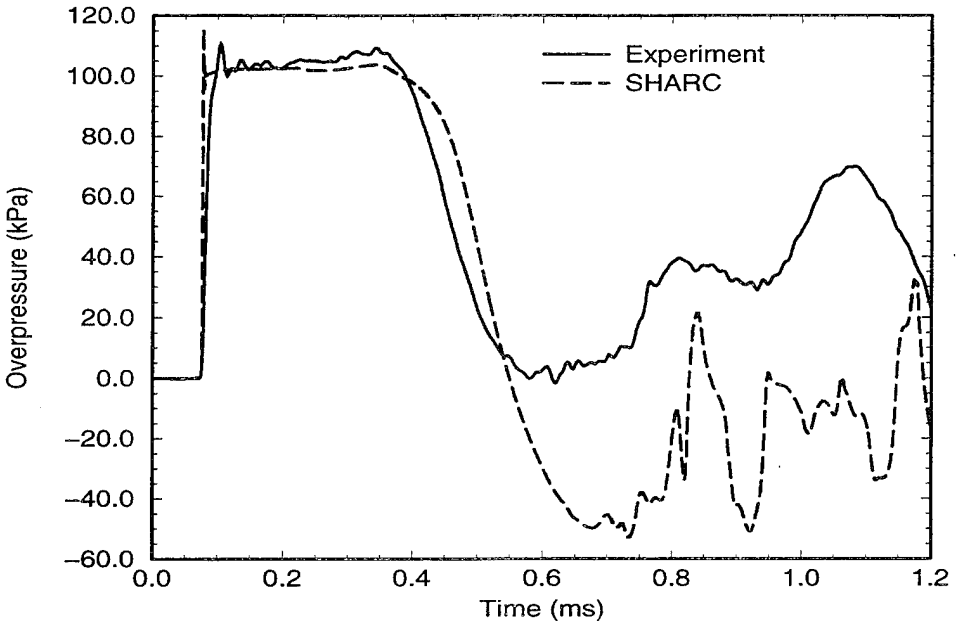

Figure 11. $M_s = 1.362$, Top Face, SHARC: Second Order, 522x294 Grid

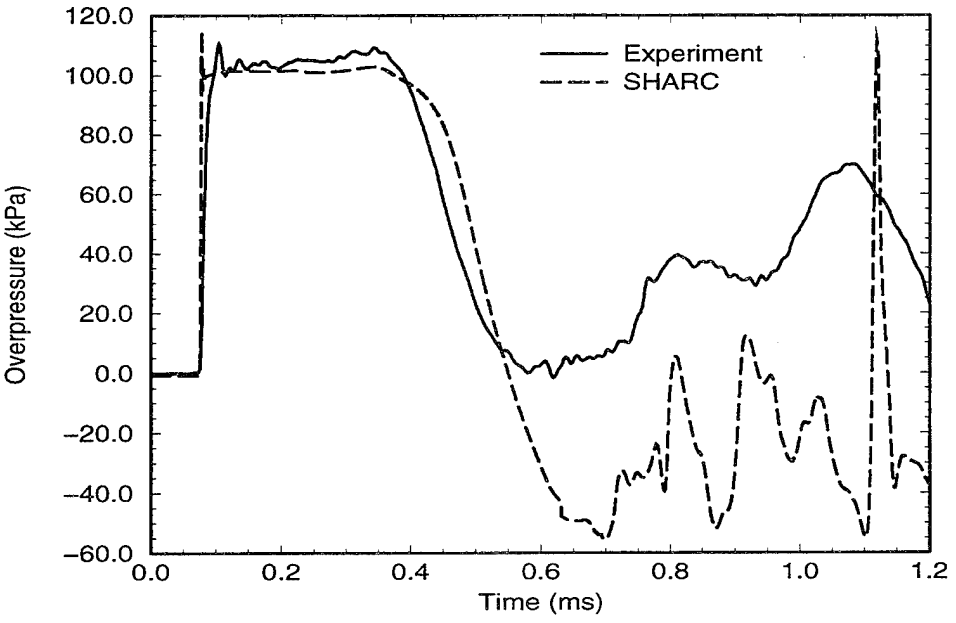

Figure 12. $M_s = 1.362$, Top Face, SHARC: Second Order, 522x652 Grid

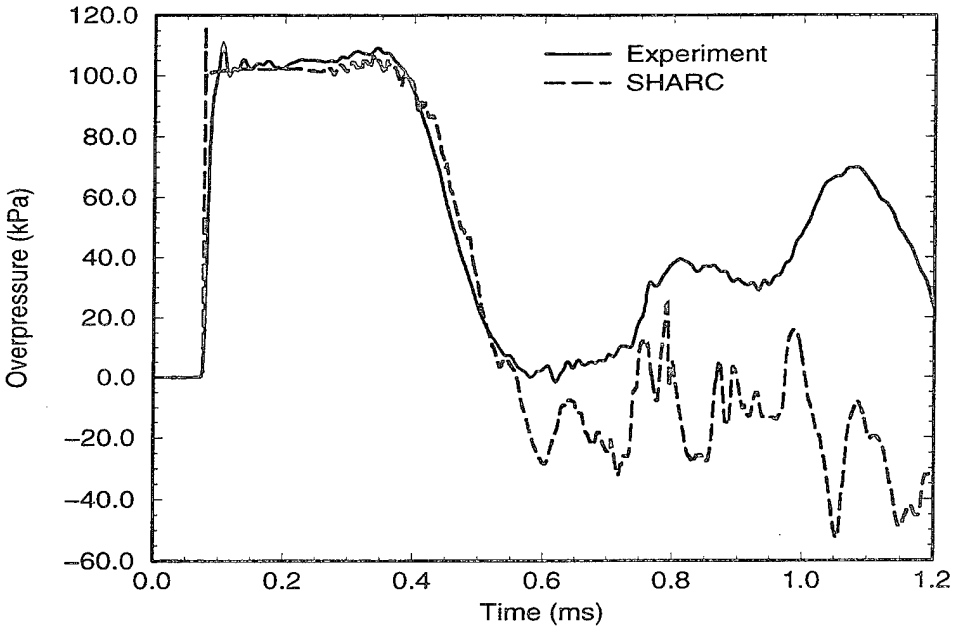

Figure 13. $M_s = 1.362$, Top Face, SHARC: Second Order, 958x1072 Grid

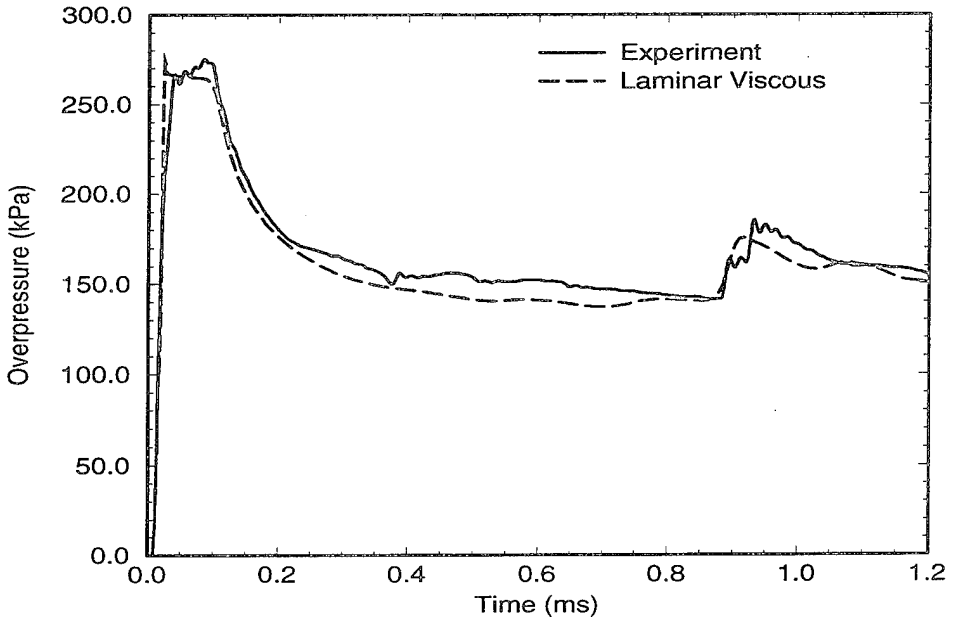

Figure 14. $M_s = 1.362$, Front Face, USA-RG2, Laminar-Viscous

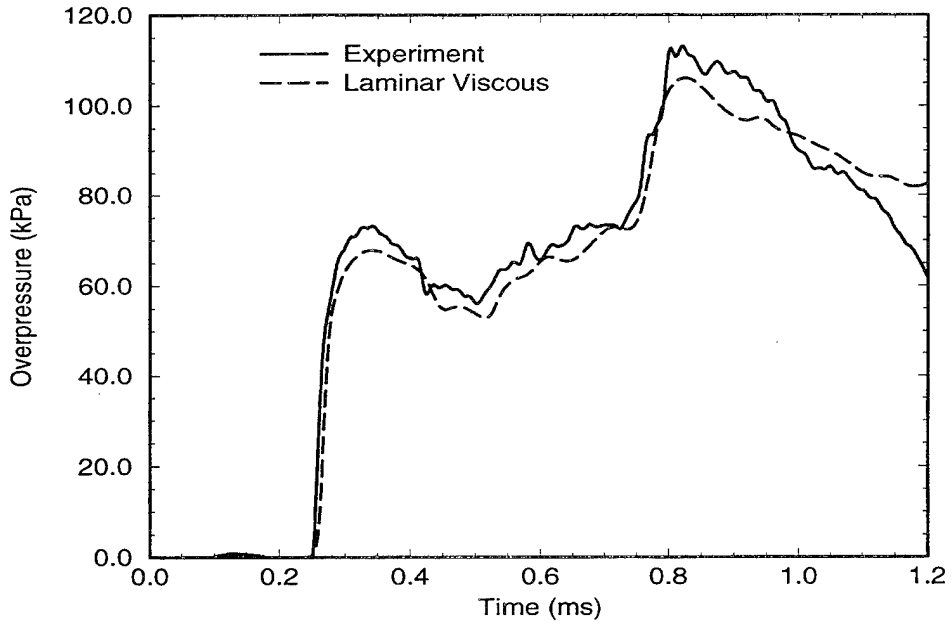

Figure 15. $M_s = 1.362$, Rear Face, USA-RG2, Laminar-Viscous

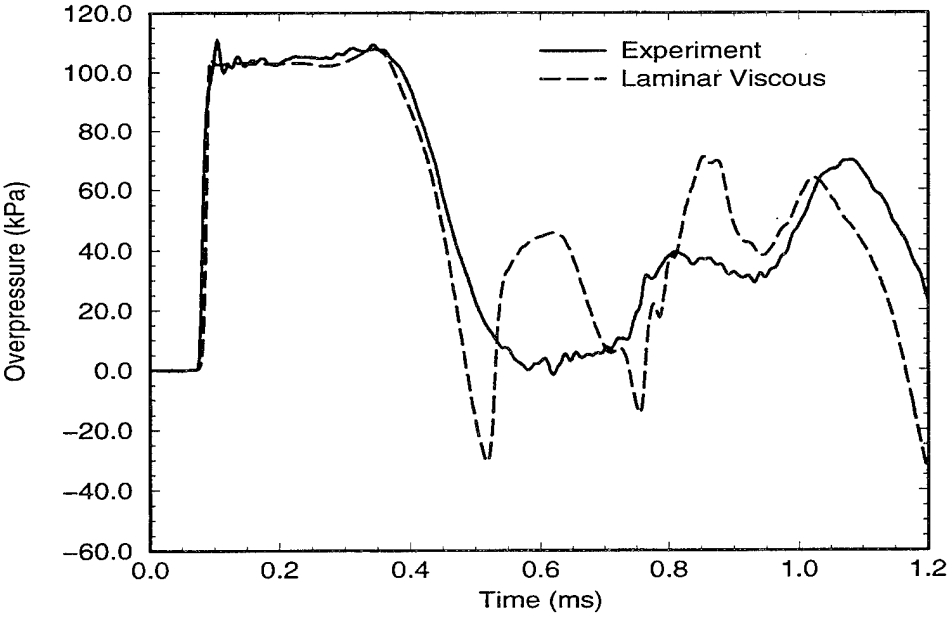

Figure 16. $M_s = 1.362$, Top Face, USA-RG2, Laminar-Viscous

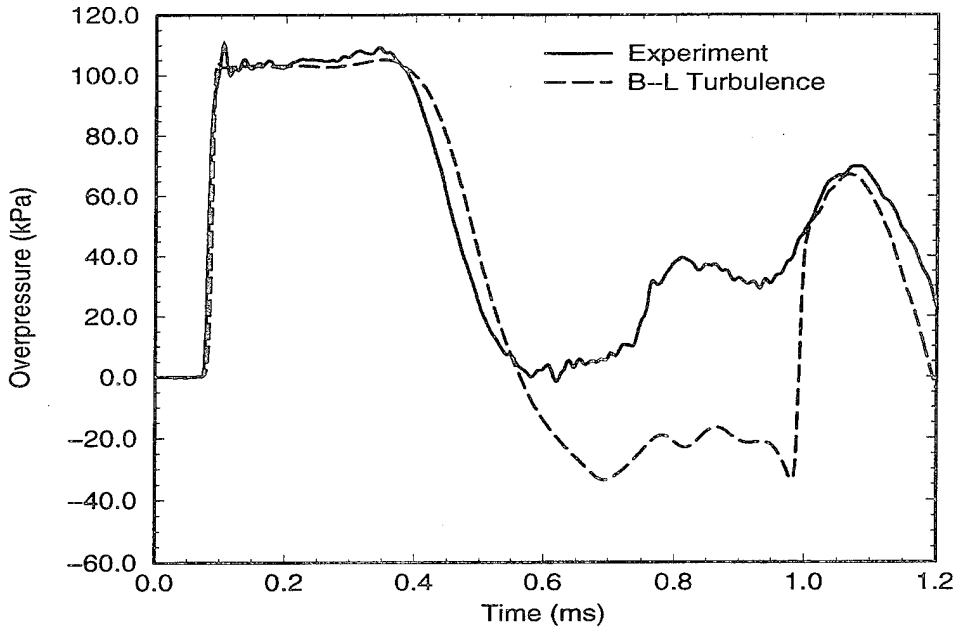

Figure 17. $M_s = 1.362$, Top Face, USA-RG2, B-L Turbulence

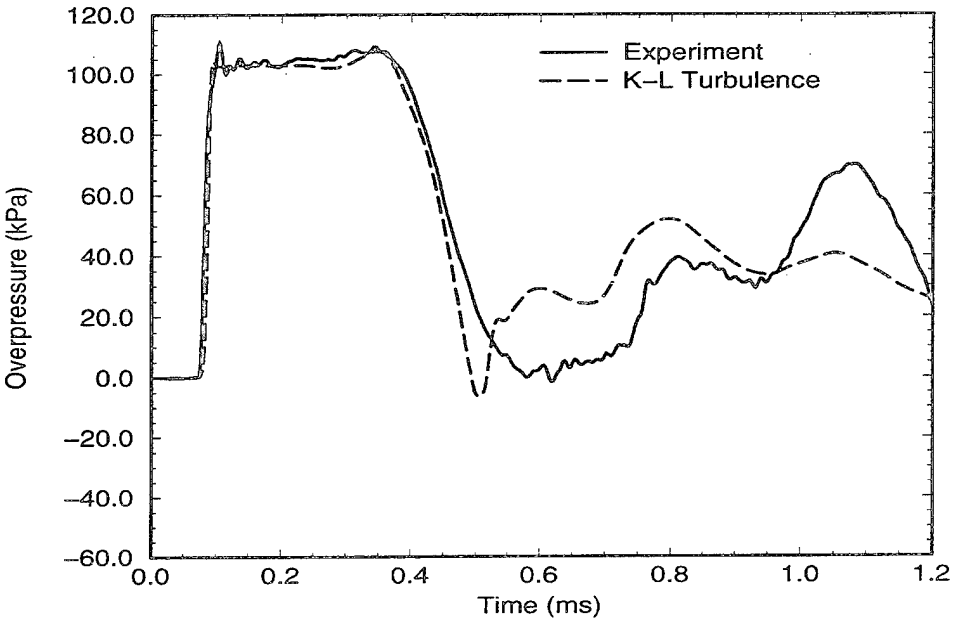

Figure 18. $M_s = 1.362$, Top Face, USA-RG2, k-L Turbulence

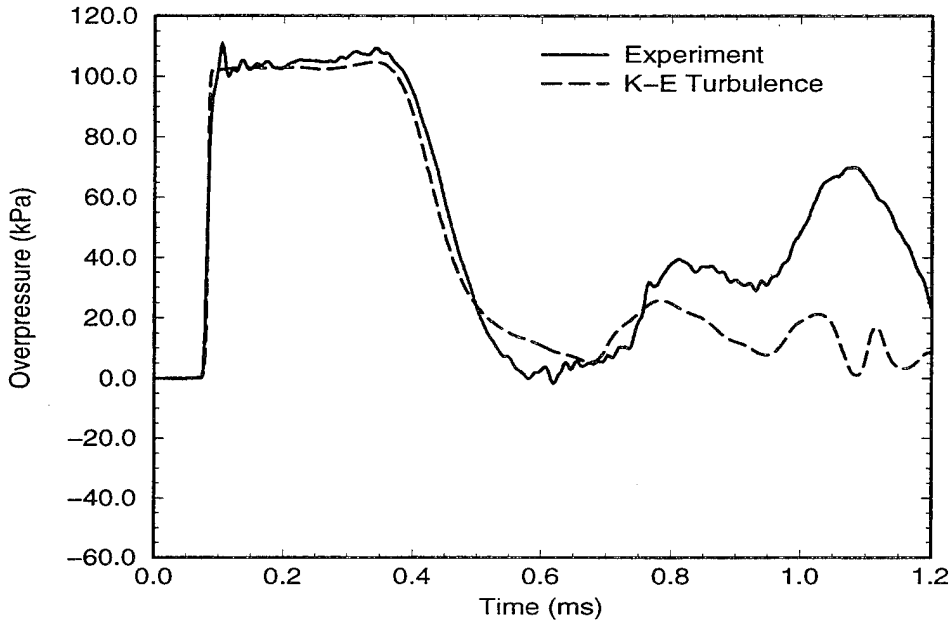

Figure 19. $M_s = 1.362$, Top Face, USA-RG2, k-ϵ Turbulence

Intentionally Left Blank

References

1. Tournemine, D. and P. Roulades. "Tube à Choc de Laboratorie Zephire - Présentation." Technical Report T-90-43. Centre d'Etudes de Gramat, France. June 1990.

2. Hikida, S., R. Bell, and C. Needham. "The SHARC Codes: Documentation and Sample Problems." S-Cubed Technical Report SSS-R-89-9878. September 1988.

3. Fry, M., R. Durret, G. Ganong, D. Matuska, M. Stucker, B. Chambers, C. Needham and C. Westmoreland. "The HULL Hydrodynamics Computer Code." U.S. Air Force Weapons Laboratory Technical Report 76-183, September 1977.

4. Barthel, J. "2-D Hydrocode Computations Using a $k - \epsilon$ Turbulence Model: Model Description and Test Calculations." S-Cubed Technical Report SSS-TR-85-7115. June 1985, (Footnotes added August 1988).

5. Chakravarthy, S., K. Szema, U. Goldberg, J. Gorski and S. Osher. "Application of a New Class of High Accuracy TVD Schemes to the Navier-Stokes Equations." AIAA Paper 85-0165. January 1985.

6. Opalka, K. "Numerical Simulation of the Flow in a 1:57-Scale Axisymmetric Model of a Large Blast Simulator." U.S. Army Research Laboratory Technical Report ARL-TR-111, Aberdeen Proving Ground, MD. April 1993.

7. Ramakrishnan, S. and U. Goldberg. "Versatility of an Algebraic Backflow Turbulence Model." AIAA Paper 90-1485. 1990

8. Goldberg, U. and S. Chakravarthy. "Separated Flow Predictions Using a Hybrid $k - L$/Backflow Model." AIAA Journal, Volume 28, Number 6. pp. 1005-1009. June 1990.

9. Goldberg, U. and D. Ota. "A $k - \epsilon$ Near-Wall Formulation for Separated Flows." AIAA Paper 90-1482. 1990.

Intentionally Left Blank

NO. OF COPIES	ORGANIZATION
2	ADMINISTRATOR DEFENSE TECHNICAL INFO CTR ATTN DTIC DDA CAMERON STATION ALEXANDRIA VA 22304-6145
1	DIRECTOR US ARMY RESEARCH LAB ATTN AMSRL OP SD TA 2800 POWDER MILL RD ADELPHI MD 20783-1145
3	DIRECTOR US ARMY RESEARCH LAB ATTN AMSRL OP SD TL 2800 POWDER MILL RD ADELPHI MD 20783-1145
1	DIRECTOR US ARMY RESEARCH LAB ATTN AMSRL OP SD TP 2800 POWDER MILL RD ADELPHI MD 20783-1145
	ABERDEEN PROVING GROUND
5	DIR USARL ATTN AMSRL OP AP L (305)

NO. OF COPIES	ORGANIZATION
2	HQDA ATTN SARD TR MS K KOMINOS DR R CHAIT WASHINGTON DC 20310-0103
2	HQDA ATTN SARD TT MS C NASH DR F MILTON WASHINGTON DC 20310-0103
2	DIRECTOR FEDERAL EMERGENCY MNGMNT AGENCY ATTN PUBLIC RELATIONS OFFICE TECHNICAL LIBRARY WASHINGTON DC 20472
1	CHAIRMAN DOD EXPLOSIVES SAFETY BOARD ROOM 856 C HOFFMAN BLDG 1 2461 EISENHOWER AVENUE ALEXANDRIA VA 22331-0600
1	DIRECTOR OF DEFENSE RESEARCH AND ENGINEERING ATTN DD TWP WASHINGTON DC 20301
1	DIRECTOR DEFENSE INTELLIGENCY AGENCY ATTN DT 2 WPNS & SYS DIVISION WASHINGTON DC 20301
1	ASSISTANT SECRETARY OF DEFENSE ATOMIC ENERGY ATTN DOCUMENT CONTROL WASHINGTON DC 20301
9	DIRECTOR DEFENSE NUCLEAR AGENCY ATTN CSTI TECHNICAL LIBRARY DDIR DFSP NANS OPNA SPSD SPTD DFTD TDTR WASHINGTON DC 20305

NO. OF COPIES	ORGANIZATION
1	CHAIRMAN JOINT CHIEFS OF STAFF ATTN J5 R&D DIVISION WASHINGTON DC 20301
2	DA DCSOPS ATTN TECHNICAL LIBRARY DIR OF CHEM & NUC OPS WASHINGTON DC 20310
3	COMMANDER FIELD COMMAND DNA ATTN FCPR FCTMOF NMHE KIRTLAND AFB NM 87115
1	U S ARMY RESEARCH DEVELOPMENT AND STANDARDIZATION GROUP UK ATTN DR ROY E REICHENBACH PSC 802 BOX 15 FPO AE 09499-1500
10	CENTRAL INTELLIGENCE AGENCY DIR DB STANDARD ATTN GE 47 HQ WASHINGTON DC 20505
1	DIRECTOR ADVANCED RESEARCH PROJECTS AGENCY ATTN TECHNICAL LIBRARY 3701 NORTH FAIRFAX DRIVE ARLINGTON VA 22203-1714
2	COMMANDER US ARMY NRDEC ATTN AMSNA D DR D SIELING STRNC UE J CALLIGEROS NATICK MA 01762
2	COMMANDER US ARMY CECOM ATTN AMSEL RD AMSEL RO TPPO P FT MONMOUTH NJ 07703-5301
1	COMMANDER US ARMY CECOM R&D TECHNICAL LIBRARY ATTN ASQNC ELC IS L R MYER CTR FT MONMOUTH NJ 07703-5000

NO. OF COPIES	ORGANIZATION
1	MIT ATTN TECHNICAL LIBRARY CAMBRIDGE MA 02139
1	COMMANDER US ARMY NGIC ATTN RESEARCH & DATA BRANCH 220 7TH STREET NE CHARLOTTESVILLE VA 22901-5396
1	COMMANDER US ARMY ARDEC ATTN SMCAR FSM W BARBER BLDG 94 PICATINNY ARSENAL NJ 07806-5000
1	DIRECTOR US ARMY TRAC FT LEE ATTN ATRC L MR CAMERON FT LEE VA 23801-6140
1	US ARMY MISSILE & SPACE INTELLIGENCE CENTER ATTN AIAMS YDL REDSTONE ARSENAL AL 35898-5500
1	COMMANDING OFFICER CODE L51 NAVAL CIVIL ENGINEERING LABORATORY ATTN J TANCRETO PORT HUENEME CA 93043-5003
2	COMMANDER US ARMY STRATEGIC DEFENSE COMMAND ATTN CSSD H MPL TECH LIB CSSD H XM DR DAVIES PO BOX 1500 HUNTSVILLE AL 35807
3	COMMANDER US ARMY CORPS OF ENGINEERS WATERWAYS EXPERIMENT STATION ATTN CEWES SS R J WATT CEWES SE R J INGRAM CEWES TL TECH LIBRARY PO BOX 631 VICKSBURG MS 39180-0631
1	COMMANDER US ARMY ENGINEER DIVISION ATTN HNDED FD PO BOX 1500 HUNTSVILLE AL 35807

NO. OF COPIES	ORGANIZATION
3	COMMANDER US ARMY NUCLEAR & CHEMICAL AGENCY 7150 HELLER LOOP SUITE 101 SPRINGFIELD VA 22150-3198
1	COMMANDER US ARMY CORPS OF ENGINEERS FT WORTH DISTRICT ATTN CESWF PM J PO BOX 17300 FT WORTH TEXAS 76102-0300
1	DIRECTOR TRAC FLVN ATTN ATRC FT LEAVENWORTH KS 66027-5200
1	COMMANDER US ARMY RESEARCH OFFICE ATTN SLCRO D PO BOX 12211 RESEARCH TRIANGLE PARK NC 27709-2211
1	COMMANDER NAVAL ELECTRONIC SYSTEMS COMMAND ATTN PME 117 21A WASHINGTON DC 20360
1	DIRECTOR HQ TRAC RPD ATTN ATRC RPR RADDA FT MONROE VA 23651-5143
2	OFFICE OF NAVAL RESEARCH ATTN DR A FAULSTICK CODE 23 800 N QUINCY STREET ARLINGTON VA 22217
1	DIRECTOR TRAC WSMR ATTN ATRC WC KIRBY WSMR NM 88002-5502
1	COMMANDER NAVAL SEA SYSTEMS COMMAND ATTN CODE SEA 62R DEPARTMENT OF THE NAVY WASHINGTON DC 20362-5101

NO. OF COPIES	ORGANIZATION
1	COMMANDER US ARMY WSMR ATTN STEWS NED DR MEASON WSMR NM 88002-5158
2	CHIEF OF NAVAL OPERATIONS DEPARTMENT OF THE NAVY ATTN OP 03EG OP 985F WASHINGTON DC 20350
1	COMMANDER DAVID TAYLOR RESEARCH CENTER ATTN CODE 522 TECH INFO CTR BETHESDA MD 20084-5000
1	OFFICER IN CHARGE CODE L31 CIVIL ENGINEERING LABORATORY NAVAL CONSTRUCTION BATTALION CTR ATTN TECHNICAL LIBRARY PORT HUENEME CA 93041
1	COMMANDING OFFICER WHITE OAK WARFARE CENTER ATTN CODE WA501 NNPO SILVER SPRING MD 20902-5000
1	COMMANDER CODE 533 NAVAL WEAPONS CENTER ATTN TECHNICAL LIBRARY CHINA LAKE CA 93555-6001
1	COMMANDER DAHLGREN DIVISION NAVAL SURFACE WARFARE CENTER ATTN CODE E23 LIBRARY DAHLGREN VA 22448-5000
1	COMMANDER NAVAL RESEARCH LABORATORY ATTN CODE 2027 TECHNICAL LIBRARY WASHINGTON DC 20375
1	OFFICER IN CHARGE WHITE OAK WARFARE CTR DETACHMENT ATTN CODE E232 TECHNICAL LIBRARY 10901 NEW HAMPSHIRE AVENUE SILVER SPRING MD 20903-5000
1	AL LSCF ATTN J LEVINE EDWARDS AFB CA 93523-5000

NO. OF COPIES	ORGANIZATION
1	COMMANDER NAVAL WEAPONS EVALUATION FAC ATTN DOCUMENT CONTROL KIRTLAND AFB NM 87117
1	RADC EMTLD DOCUMENT LIBRARY GRIFFISS AFB NY 13441
1	AEDC ARNOLD AFB TN 37389
1	AFESC RDCS ATTN PAUL ROSENGREN TYNDALL AFB FL 32403
1	OLAC PL TSTL ATTN D SHIPLETT EDWARDS AFB CA 93523-5000
1	AFIT ENY ATTN LTC HASEN PHD WRIGHT PATTERSON AFB OH 45433-6583
2	AIR FORCE ARMAMENT LABORATORY ATTN AFATL DOIL AFATL DLYV EGLIN AFB FL 32542-5000
1	DIRECTOR IDAHO NATIONAL ENGINEERING LAB ATTN SPEC PROGRAMS J PATTON 2151 NORTH BLVD MS 2802 IDAHO FALLS ID 83415
3	PHILLIPS LABORATORY AFWL ATTN NTE NTED NTES KIRTLAND AFB NM 87117-6008
1	DIRECTOR LAWRENCE LIVERMORE NATIONAL LAB ATTN TECH INFO DEPT L 3 PO BOX 808 LIVERMORE CA 94550
1	AFIT ATTN TECHNICAL LIBRARY BLDG 640 B WRIGHT PATTERSON AFB OH 45433

NO. OF COPIES	ORGANIZATION
1	DIRECTOR NATIONAL AERONAUTICS & SPACE ADMIN ATTN SCIENTIFIC & TECH INFO FAC PO BOX 8757 BWI AIRPORT BALTIMORE MD 21240
1	FTD NIIS WRIGHT PATTERSON AFB OH 45433
3	KAMAN SCIENCES CORPORATION ATTN LIBRARY PA ELLIS FH SHELTON PO BOX 7463 COLORADO SPRINGS CO 80933-7463
4	DIRECTOR IDAHO NATIONAL ENGINEERING LAB EG&G IDAHO INC ATTN R GUENZLER MS 3505 R HOLMAN MS 3510 R A BERRY W C REED PO BOX 1625 IDAHO FALLS ID 83415
5	DIRECTOR SANDIA NATIONAL LABS ATTN DOC CONTROL 3141 C CAMERON DIV 6215 A CHABAI DIV 7112 D GARDNER DIV 1421 J MCGLAUN DIV 1541 PO BOX 5800 ALBUQUERQUE NM 87185-5800
2	DIRECTOR LOS ALAMOS NATIONAL LABORATORY ATTN TH DOWLER MS F602 DOC CONTROL FOR REPORTS LIBRARY PO BOX 1663 LOS ALAMOS NM 87545
1	BLACK & VEATCH ENGINEERS ARCHITECTS ATTN HD LAVERENTZ 1500 MEADOW LAKE PARKWAY KANSAS CITY MO 64114

NO. OF COPIES	ORGANIZATION
1	DIRECTOR SANDIA NATIONAL LABORATORIES LIVERMORE LABORATORY ATTN DOC CONTROL FOR TECH LIB PO BOX 969 LIVERMORE CA 94550
1	DIRECTOR NASA AMES RESEARCH CENTER APPLIED COMPUTATIONAL AERO BRANCH ATTN DR T HOLTZ MS 202 14 MOFFETT FIELD CA 94035
1	DIRECTOR NASA LANGLEY RESEARCH CENTER ATTN TECHNICAL LIBRARY HAMPTON VA 23665
2	APPLIED RESEARCH ASSOCIATES INC ATTN J KEEFER NH ETHRIDGE PO BOX 548 ABERDEEN MD 21001
1	ADA TECHNOLOGIES INC ATTN JAMES R BUTZ HONEYWELL CENTER SUITE 110 304 INVERNESS WAY SOUTH ENGLEWOOD CO 80112
1	ALLIANT TECHSYSTEMS INC ATTN ROGER A RAUSCH MN48 3700 7225 NORTHLAND DRIVE BROOKLYN PARK MN 55428
1	CARPENTER RESEARCH CORPORATION ATTN H JERRY CARPENTER 27520 HAWTHORNE BLVD SUITE 263 PO BOX 2490 ROLLING HILLS ESTATES CA 90274
1	AEROSPACE CORPORATION ATTN TECH INFO SERVICES PO BOX 92957 LOS ANGELES CA 90009
1	GOODYEAR CORPORATION ATTN RM BROWN BLDG 1 SHELTER ENGINEERING LITCHFIELD PARK AZ 85340

NO. OF COPIES	ORGANIZATION
1	THE BOEING COMPANY ATTN AEROSPACE LIBRARY PO BOX 3707 SEATTLE WA 98124
2	FMC CORPORATION ADVANCED SYSTEMS CENTER ATTN J DROTLEFF C KREBS MDP 95 BOX 58123 2890 DE LA CRUZ BLVD SANTA CLARA CA 95052
1	CALIFORNIA RES & TECH INC ATTN M ROSENBLATT 20943 DEVONSHIRE STREET CHATSWORTH CA 91311
1	SVERDRUP TECHNOLOGY INC SVERDRUP CORPORATION AEDC ATTN BD HEIKKINEN MS 900 ARNOLD AFB TN 37389-9998
1	DYNAMICS TECHNOLOGY INC ATTN D T HOVE G P MASON 21311 HAWTHORNE BLVD SUITE 300 TORRANCE CA 90503
1	KTECH CORPORATION ATTN DR E GAFFNEY 901 PENNSYLVANIA AVE NE ALBUQUERQUE NM 87111
1	EATON CORPORATION DEFENSE VALVE & ACTUATOR DIV ATTN J WADA 2338 ALASKA AVE EL SEGUNDO CA 90245-4896
2	MCDONNELL DOUGLAS ASTRONAUTICS CORP ATTN ROBERT W HALPRIN KA HEINLY 5301 BOLSA AVENUE HUNTINGTON BEACH CA 92647

NO. OF COPIES	ORGANIZATION
4	KAMAN AVIDYNE ATTN R RUETENIK 2 CP S CRISCIONE R MILLIGAN 83 SECOND AVENUE NORTHWEST INDUSTRIAL PARK BURLINGTON MA 01830
1	MDA ENGINEERING INC ATTN DR DALE ANDERSON 500 EAST BORDER STREET SUITE 401 ARLINGTON TX 07601
2	PHYSICS INTERNATIONAL CORPORATION PO BOX 5010 SAN LEANDRO CA 94577-0599
2	KAMAN SCIENCES CORPORATION ATTN DASIAC 2 CP PO DRAWER 1479 816 STATE STREET SANTA BARBARA CA 93102-1479
1	R&D ASSOCIATES ATTN GP GANONG PO BOX 9377 ALBUQUERQUE NM 87119
1	LOCKHEED MISSILES & SPACE CO ATTN J J MURPHY DEPT 81 11 BLDG 154 PO BOX 504 SUNNYVALE CA 94086
2	SCIENCE CENTER ROCKWELL INTERNATIONAL CORP ATTN DR S CHAKRAVARTHY DR D OTA 1049 CAMINO DOS RIOS THOUSAND OAKS CA 91358
1	ORLANDO TECHNOLOGY INC ATTN D MATUSKA 60 SECOND STREET BLDG 5 SHALIMAR FL 32579

NO. OF COPIES	ORGANIZATION
3	S CUBED A DIVISION OF MAXWELL LABS INC ATTN TECHNICAL LIBRARY R DUFF K PYATT PO BOX 1620 LA JOLLA CA 92037-1620
2	THE RALPH M PARSONS COMPANY ATTN T M JACKSON LB TS PROJECT MANAGER 100 WEST WALNUT STREET PASADENA CA 91124
1	SAIC ATTN J GUEST 2301 YALE BLVD SE SUITE E ALBUQUERQUE NM 87106
1	SUNBURST RECOVERY INC ATTN DR C YOUNG PO BOX 2129 STEAMBOAT SPRINGS CO 80477
1	SAIC ATTN N SINHA 501 OFFICE CENTER DRIVE APT 420 FT WASHINGTON PA 19034-3211
1	SVERDRUP TECHNOLOGY INC ATTN RF STARR PO BOX 884 TULLAHOMA TN 37388
2	S CUBED A DIVISION OF MAXWELL LABS INC ATTN C E NEEDHAM L KENNEDY 2501 YALE BLVD SE ALBUQUERQUE NM 87106
3	SRI INTERNATIONAL ATTN DR GR ABRAHAMSON DR J GRAN DR B HOLMES 333 RAVENWOOD AVENUE MENLO PARK CA 94025

NO. OF COPIES	ORGANIZATION
1	TRW BALLISTIC MISSILE DIVISION ATTN H KORMAN MAIL STATION 526 614 PO BOX 1310 SAN BERNADINO CA 92402
1	BATTELLE TWSTIAC 505 KING AVENUE COLUMBUS OH 43201-2693
1	THERMAL SCIENCE INC ATTN R FELDMAN 2200 CASSENS DRIVE ST LOUIS MO 63026
2	DENVER RESEARCH INSTITUTE ATTN J WISOTSKI TECHNICAL LIBRARY PO BOX 10758 DENVER CO 80210
1	STATE UNIVERSITY OF NEW YORK MECHANICAL & AEROSPACE ENGINEERING ATTN DR PEYMAN GIVI BUFFALO NY 14260
2	UNIVERSITY OF MARYLAND INSTITUTE FOR ADV COMPUTER STUDIES ATTN L DAVIS G SOBIESKI COLLEGE PARK MD 20742
2	THINKING MACHINES CORPORATION ATTN G SABOT R FERREL 245 FIRST STREET CAMBRIDGE MA 02142-1264
1	NORTHROP UNIVERSITY ATTN DR FB SAFFORD 5800 W ARBOR VITAE STREET LOS ANGELES CA 90045
1	CALIFORNIA INSTITUTE OF TECHNOLOGY ATTN T J AHRENS 1201 E CALIFORNIA BLVD PASADENA CA 91109

NO. OF COPIES	ORGANIZATION
1	STANFORD UNIVERSITY ATTN DR D BERSHADER DURAND LABORATORY STANFORD CA 94305
1	UNIVERSITY OF MINNESOTA ARMY HIGH PERF COMP RES CTR ATTN DR TAYFUN E TEZDUYAR 1100 WASHINGTON AVE SOUTH MINNEAPOLIS MN 55415
3	SOUTHWEST RESEARCH INSTITUTE ATTN DR C ANDERSON S MULLIN A B WENZEL PO DRAWER 28255 SAN ANTONIO TX 78228-0255
2	COMMANDER US ARMY NRDEC ATTN SSCNC YSD J ROACH SSCNC WST A MURPHY KANSAS STREET NATICK MA 10760-5018

NO. OF COPIES	ORGANIZATION
	ABERDEEN PROVING GROUND
1	CDR USATECOM ATTN AMSTE TE F L TELETSKI
1	CDR USATHAMA ATTN AMSTH TE
1	CDR USATC ATTN STEC LI
26	DIR USARL ATTN AMSRL SC C H BREAUX AMSRL SC CC C NIETUBICZ C ELLIS D HISLEY N PATEL T KENDALL R SHEROKE AMSRL SC I W STUREK AMSRL SC AE M COLEMAN AMSRL SC S R PEARSON AMSRL SL CM E FIORVANTE AMSRL WT N J INGRAM AMSRL WT NA R KEHS AMSRL WT NC R LOTTERO B MCGUIRE A MIHALCIN P MULLER R LOUCKS S SCHRAML AMSRL WT ND J MILETTA AMSRL WT NF L JASPER AMSRL WT NG T OLDHAM AMSRL WT NH J CORRIGAN AMSRL WT PB P WEIHNACHT B GUIDOS AMSRL WT TC K KIMSEY

USER EVALUATION SHEET/CHANGE OF ADDRESS

This Laboratory undertakes a continuing effort to improve the quality of the reports it publishes. Your comments/answers to the items/questions below will aid us in our efforts.

1. ARL Report Number ARL-TR-848 Date of Report September 1995

2. Date Report Received _____

3. Does this report satisfy a need? (Comment on purpose, related project, or other area of interest for which the report will be used.) _____

_____

_____

4. Specifically, how is the report being used? (Information source, design data, procedure, source of ideas, etc.)

_____

_____

_____

5. Has the information in this report led to any quantitative savings as far as man-hours or dollars saved, operating costs avoided, or efficiencies achieved, etc? If so, please elaborate. _____

_____

_____

6. General Comments. What do you think should be changed to improve future reports? (Indicate changes to organization, technical content, format, etc.) _____

_____

_____

_____

CURRENT ADDRESS

_____
Organization

_____
Name

_____
Street or P.O. Box No.

_____
City, State, Zip Code

7. If indicating a Change of Address or Address Correction, please provide the Current or Correct address above and the Old or Incorrect address below.

OLD ADDRESS

_____
Organization

_____
Name

_____
Street or P.O. Box No.

_____
City, State, Zip Code

(Remove this sheet, fold as indicated, tape closed, and mail.)

(DO NOT STAPLE)

DEPARTMENT OF THE ARMY

OFFICIAL BUSINESS

NO POSTAGE
NECESSARY
IF MAILED
IN THE
UNITED STATES

BUSINESS REPLY MAIL
FIRST CLASS PERMIT NO 0001,APG,MD

POSTAGE WILL BE PAID BY ADDRESSEE

DIRECTOR
U.S. ARMY RESEARCH LABORATORY
ATTN: AMSRL-WT-NC
ABERDEEN PROVING GROUND, MD 21005-5066